PHYSICAL REVIEW B, VOLUME 64, 184404

Strain effect and the phase diagram of $La_{1-x}Ba_xMnO_3$ thin films

Jun Zhang, Hidekazu Tanaka, Teruo Kanki, Jae-Hyoung Choi, and Tomoji Kawai*
Institute of Scientific and Industrial Research, Osaka University, 8-1 Mihogaoka, Ibaraki, Osaka, 567-0047, Japan

(Received 16 April 2001; published 12 October 2001)

We report magnetic and transport properties of $La_{1-x}Ba_xMnO_3$ ($x=0.05$–0.33) epitaxial thin films. Compared with the corresponding bulk materials, the ferromagnetic transition temperature is reduced in the compressive strained $La_{1-x}Ba_xMnO_3$ thin films with $x=0.3$ and 0.33, but enhanced significantly in the tensile strained thin films with $x \leqslant 0.2$. Especially, ferromagnetism and low field colossal magnetoresistance effect were observed around room temperature in $x=0.1$ thin film, and as $x=0.05$, a spin-canting insulating state in bulk shifts to ferromagnetic metallic state in thin film. The phase diagram of $La_{1-x}Ba_xMnO_3$ thin films was obtained, and strain effect on these novel properties was discussed.

DOI: 10.1103/PhysRevB.64.184404 PACS number(s): 75.70.Ak, 75.30.Kz, 71.30.+h, 75.30.Vn

I. INTRODUCTION

Since the observation of colossal magnetoresistance (CMR) effect in doped manganese oxides $La_{1-x}A_xMnO_3$ (where A is divalent ions, such as Ca, Sr, and Ba), they have been extensively investigated. CMR thin films are of special interest due to their advantages in practical applications. In addition to the dominant parameters as in bulk materials, including A ion size and doping level x, biaxial strain due to lattice mismatch between film and substrate plays a very important role in controlling the properties of thin films, especially Curie temperature, magnetic anisotropy and transport properties.[1–6] Strained CMR thin films usually show properties much different from those of bulk compounds. In most cases, tensile strain suppresses ferromagnetism and reduces ferromagnetic (FM) Curie temperature T_C in CMR thin films, which is generally interpreted by considering a strain-induced distortion of MnO_6 octahedra.[5–6] But some anomalous results[7–8] have also been reported, showing ferromagnetism enhanced by tensile strain. Notably, some novel properties[9–10] were observed in CMR thin films, indicating that strain effect can be utilized to tailor or optimize the magnetotransport properties of CMR thin films, although a thorough understanding of strain effect is still unavailable and challenging.

Although $La_{1-x}Ba_xMnO_3$ (denoted as LBMO hereafter) show room-temperature CMR effect[11] and higher T_C in low doping level than other CMR systems,[12] little research has focused on this CMR material, especially the LBMO thin films. Recently, it was reported that in $La_{2/3}Ba_{1/3}MnO_3/SrTiO_3$ superlattices,[13] compressive strain reduces T_C but enhances CMR. Most notably, Kanki *et al.*[14] found that both T_C and CMR effect are enhanced in tensile strained $La_{0.8}Ba_{0.2}MnO_3/SrTiO_3$ thin films. This result is different from the usual ones in other well studied CMR thin films, and suggests that there is an anomalous strain effect, which may induce some novel and interesting properties in LBMO thin films. A detailed study of the strained LBMO thin films may help us go further in wholly understanding strain effect.

In this paper we report a systematic investigation of magnetic and transport properties in the strained LBMO thin films with doping level x from 0.05 to 0.33, which are grown on $SrTiO_3$ (100) (denoted as STO hereafter) substrate. By comparing the lattice parameters of LBMO targets and STO substrate ($a=3.905$ Å), the lattice mismatches in LBMO/STO thin films can be derived (listed in Table I), and indicate that the LBMO films suffer tensile strain (negative lattice mismatch) as $x \leqslant 0.2$, but compressive strain (positive lattice mismatch) as $x=0.3$ and 0.33. With x increasing, tensile strain becomes weaker, then converts to compressive strain as x exceeding 0.2, which enables us to investigate the strain effect in detail and systematically without changing substrate. We found that in LBMO thin films, tensile strain enhances ferromagnetism significantly, but compressive strain reduces T_C. In particular, room-temperature ferromagnetism was observed in LBMO thin film with a very low doping level of $x=0.1$, which will endow it high superiority in applications of electronic devices. In addition, a new phase diagram of LBMO thin films was constructed.

II. EXPERIMENT

LBMO films ($x=0.05$–0.33) were deposited on STO (100) single crystal substrates by pulsed laser deposition technique (ArF excimer: $\lambda=193$ nm). LBMO targets were prepared by a standard solid state reaction. LBMO films were deposited at a substrate temperature of 730 °C and an oxygen pressure of 0.1 Pa, and post-annealed in 1 atm oxygen at 700 to 900 °C for 10 h to avoid any oxygen deficiency.

TABLE I. Lattice mismatch, strain type (T: tensile strain; C: compressive strain), and T_C of LBMO/STO thin films, as well as T_C of the bulk LBMO. Lattice mismatch was calculated as the difference between the lattice parameters of LBMO bulk and STO substrate divided by the lattice parameter of STO ($a_0=3.905$ Å). T_C was defined as the temperature where dM/dT is the minimum in the M-T curves shown in Fig. 3.

x	0.05	0.1	0.2	0.3	0.33
Lattice mismatch (%)	−0.76	−0.63	−0.29	0.1	0.15
Strain type	T	T	T	C	C
T_C of bulk (K)	120[a]	185	280	340	345
T_C of film (20 nm) (K)	180	285	310	290	315

[a] For $x=0.05$, spin canting transition temperature $T_{CA}=120$ K.

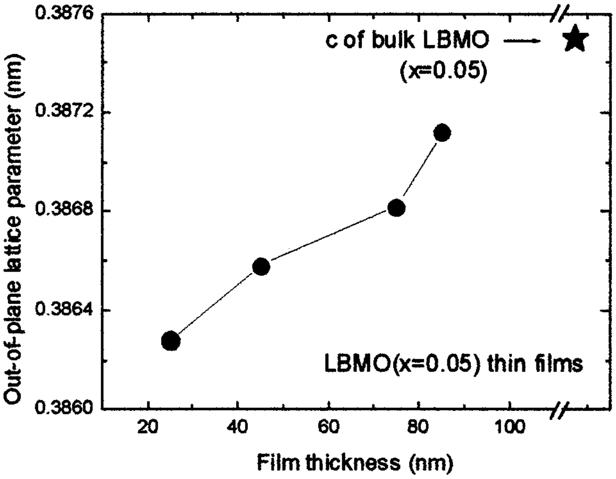

FIG. 1. Thickness dependence of out-of-plane lattice parameter for LBMO $(x=0.05)$ thin films. The star symbol represents the lattice parameter c value of bulk LBMO $(x=0.05)$.

The film structures were studied by reflection high energy electron diffraction (RHEED), x-ray diffraction (XRD), and high-resolution transmission electron microscopy (HRTEM, JEOL JEM 3000FIS, operating at 300 kV). The magnetization of LBMO bulk and thin films were measured by using a SQUID magnetometer (Quantum Design). Resistivities of thin films were measured along in-plane direction by standard four-probe method.

III. RESULTS AND DISCUSSION

A. Structure analysis

The RHEED images of LBMO thin films showed clear streak patterns, suggesting good crystalline and flat surface of the films.[14,15] Only $(00l)$ peaks were observed in XRD patterns, indicating that the LBMO films are well c oriented and epitaxial. The bulk LBMO could be considered as a pseudocubic structure. As being deposited on STO, the in-plane lattice tends to adopt the same structure as STO, and the out-of-plane parameter changes correspondingly to maintain unit cell volume. The out-of-plane lattice parameter of LBMO thin films derived from XRD data is found to be larger than the bulk parameter in compressive strain range, but smaller in tensile strain range, in line with the type of biaxial strain. In Fig. 1, we show the thickness dependence of out-of-plane lattice parameter for LBMO thin films with $x=0.05$, which have the largest lattice mismatch in the studied system. The out-of-plane lattice parameter of thin films is smaller than the c value of bulk, in agreement with the existence of tensile strain, which will elongate the in-plane parameter and shorten the out-of-plane parameter. The smaller c confirmed the existence of tensile strain in the annealed thin films. With thickness increasing, the out-of-plane lattice parameter increases and approaches the bulk value, indicating a relaxing or weakening of tensile strain in the films.

TEM analysis on the cross-sectional specimens revealed that LBMO thin films are of epitaxial single-crystal. Figure 2(a) is a typical cross-sectional HRTEM image of one LBMO $(x=0.1)$ thin film, which demonstrates a sharp film-substrate interface denoted by arrows, without indication of any second phase. No defects, dislocations or stacking faults were observed. A typical selected area diffraction pattern (SADP) obtained from the interface region is shown in Fig. 2(b). It is clear that there is no extra spots or splitting of reflections but only $\langle 001\rangle$ zone axis pattern. These features confirmed the high crystalline quality and perfect epitaxy of LBMO thin films.

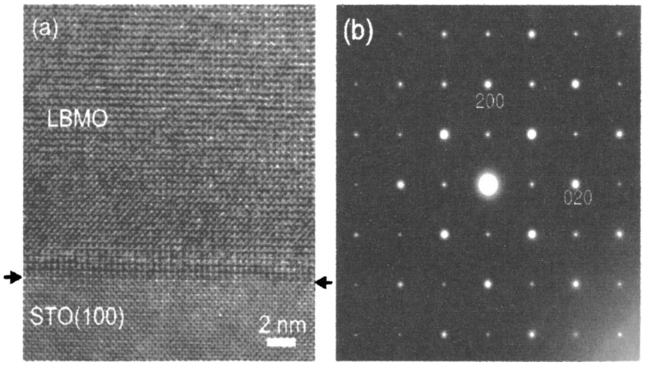

FIG. 2. (a) HRTEM image of the interface between LBMO $(x=0.1)$ thin film and STO substrate; (b) Selected area diffraction pattern along [001].

B. Magnetic properties

The temperature dependence of magnetization for LBMO bulk and thin films with thickness of 50 nm are shown in Fig. 3. For the LBMO bulk with $x=0.1$, 0.2, 0.3, and 0.33, T_C are 185, 280, 340, and 345 K, respectively, which are consistent with a previous report.[12] The $x=0.05$ bulk only shows a spin canting-like (or spin-freezing in Ref. 12) transition around 120 K, below which the zero-field cooled (ZFC) magnetization decreases and deviates greatly from the field cooled (FC) value. No spontaneous magnetization was observed in the field dependent magnetization curve shown in Fig. 4, also confirming the absence of FM order in the $x=0.05$ bulk.

Compared with the LBMO bulk, LBMO thin films show a lot of different results. As shown in Fig. 3 and Table I, in compressive strain range with higher doping levels $(x=0.3$ and 0.33), T_C in the thin films is lower than that in bulk; but for the tensile strained thin films with lower doping levels $(x=0.1$ and 0.2), T_C increases drastically. Especially, in the $x=0.1$ film with thickness of 50 nm, T_C increases remarkably from 185 K in bulk up to near room temperature (275 K). Furthermore, in the case of $x=0.05$, a spin-canting state in bulk shifts to a strong FM state in thin film, which is also revealed by the low temperature magnetization curves shown in Fig. 4. To our knowledge, this is the first time a transition from spin canting in bulk to ferromagnetic in strained thin film in CMR oxides has been reported. It is obvious that, compared with corresponding bulk compounds, ferromagnetism of LBMO thin films is suppressed in compressive strain range, but enhanced in tensile strain range. We believe that strain effect plays an important role in producing the variations of magnetic properties.

The thickness dependence of T_C for LBMO films is plotted in Fig. 5. In the tensile strain region $(x=0.05$, 0.1, and

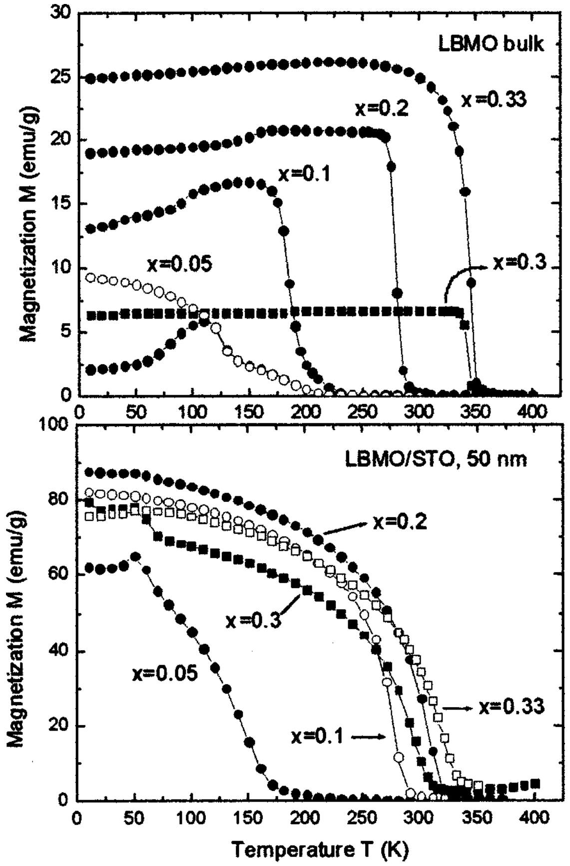

FIG. 3. Temperature dependence of magnetization for LBMO bulk samples (top graph, applied field is 200 Oe; open circle is FC data for $x=0.05$), and LBMO thin films with thickness 50 nm (bottom graph, applied field is 1000 Oe).

0.2), with thickness increasing, T_C decreases gradually and tends to approach the corresponding bulk value. In the compressive strain range, for the $x=0.3$ and 0.33 films, T_C increases slightly with thickness, which is consistent with the weak compressive strain (small lattice mismatch) in these doping levels. As mentioned above, in $x=0.05$ thin films, the out-of-plane lattice parameter increases with thickness, indicating a relaxation of the biaxial tensile strain. Same tendency of strain relaxation with thickness increasing can be expected in other doping levels. Strain relaxation weakens strain effect and results in T_C retrieving to the bulk value. The solid relationship between strain relaxation and T_C variation suggests that it is reasonable to attribute the anomalous magnetic properties of LBMO thin films to strain effect. T_C of LBMO bulk and thin films with thickness 20 nm are listed in Table I. The enhancement of ferromagnetism by tensile strain in low doping levels is very significant, and room-temperature ferromagnetism (T_C is 285 K) was observed in the $x=0.1$ thin film with thickness of 20 nm.

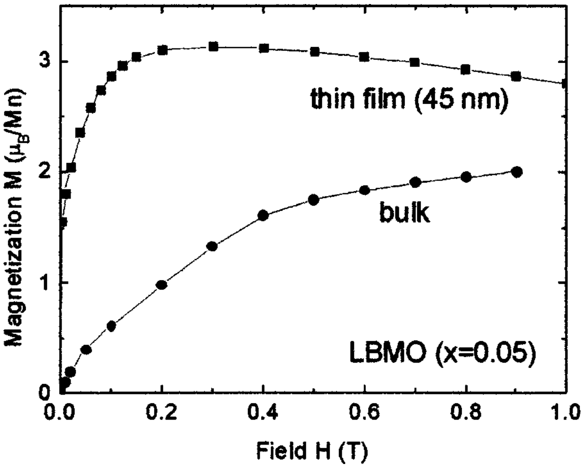

FIG. 4. Field dependence of magnetization for LBMO ($x=0.05$) bulk and thin film at 10 K.

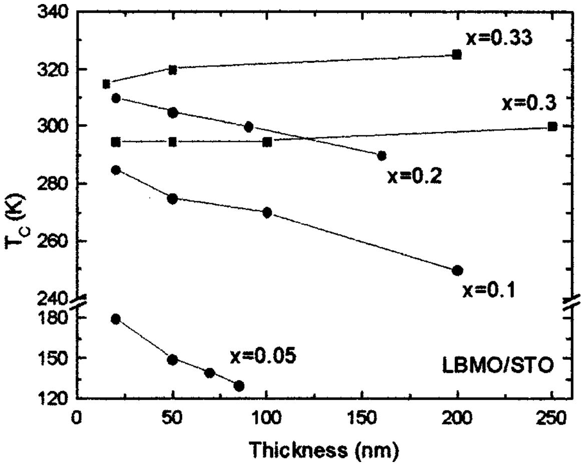

FIG. 5. T_C of LBMO thin films as a function of thickness.

C. Transport properties

Novel transport properties were also found in LBMO thin films. Figure 6 plots the temperature dependence of resistivity for $x=0.05$ LBMO bulk and thin films. The bulk shows insulating behavior with high resistivity. But for a 20 nm thin

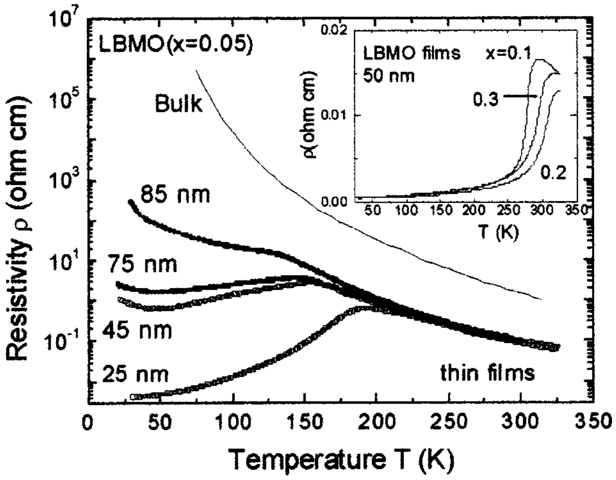

FIG. 6. Temperature dependence of resistivity for the LBMO ($x=0.05$) bulk and thin films with different thickness. Inset: temperature dependence of resistivity for LBMO thin films ($x=0.1$, 0.2, and 0.3) with thickness of 50 nm.

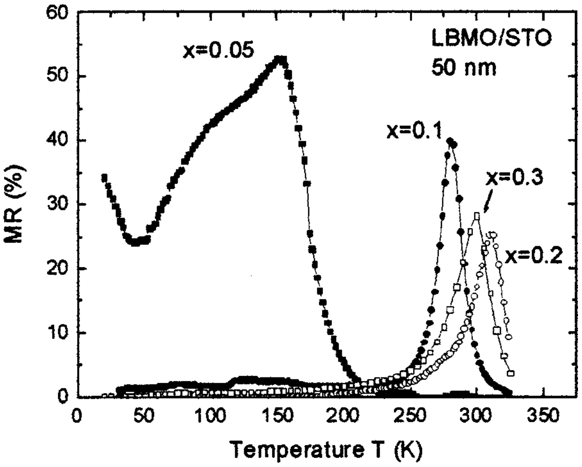

FIG. 7. Temperature dependence of magnetoresistance ratio for LBMO ($x=0.05\sim0.3$) thin films with thickness of 50 nm.

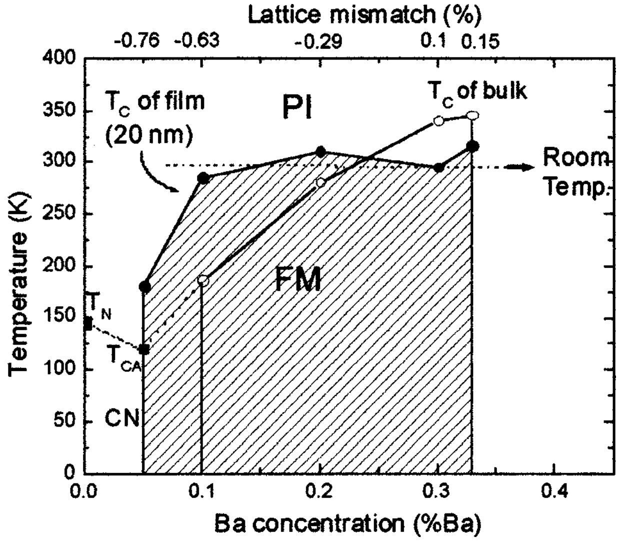

FIG. 8. Phase diagram of LBMO/STO thin films with thickness 20 nm, as well as that of LBMO bulk compounds as comparison. The lattice mismatches between LBMO and STO are also shown in top axis. FM, PI, and CNI denote ferromagnetic metallic, paramagnetic insulating, and spin canting insulating, respectively. T_N, the Neel temperature of $LaMnO_3$, is 150 K, which is generally accepted in many literatures, other than about 125 K in Ref. 12.

film, an insulating to metallic (IM) transition occurs with a peak temperature (T_{IM}) about 185 K, near T_C, and much lower resistivity, indicating much higher e_g electron itineracy. With thickness increasing, T_{IM} decreases, similar to the thickness dependence of T_C, and low temperature resistivity increases greatly. In the films with thickness of 45 and 75 nm, insulating behavior reemerges below 50 K. As thickness increases to 85 nm, IM transition disappears, with only an anomaly in resistivity curve around 125 K. The evolution of transport behavior with thickness in LBMO thin films is in good agreement with those of magnetic property and structural parameter, evidencing the strong correlation between strain effect and magnetotransport properties. It is tensile strain that enhances double exchange interaction, producing the FM and metallic state in thin film, in comparison with the spin canting and insulating state in bulk. The strain-induced transition in LBMO ($x=0.05$) from spin-canting insulating in bulk to FM metallic in thin film is very interesting, and suggests a common or similar physical essence of strain effect with/to those of pressure or magnetic field, which are well known in effectively controlling the transport properties of CMR oxides. A similar result had been reported for $La_{0.9}Sr_{0.1}MnO_3$ thin film,[10] where an IM transition was induced by compressive strain. In addition, novel transport properties were also observed in other strained CMR thin films.[8,9]

The inset in Fig. 6 shows the temperature dependence of resistivity for LBMO thin films ($x=0.1$, 0.2, and 0.3) with thickness of 50 nm. IM transitions were observed around T_C at each doping level. T_{IM} is a little higher than the corresponding T_C, and the x dependence of T_{IM} is in agreement with that of T_C as suggested by Fig. 5. It is notable that as $x=0.1$, bulk sample shows insulating behavior (not shown here), revealing that a strain-induced IM transition also happened in the $x=0.1$ LBMO thin films.

Enhanced CMR effect has been found in the $x=0.2$ LBMO thin films at or above room temperature.[14] In fact, even at a lower doping level as $x=0.1$, very strong CMR effect can be obtained around room temperature. Figure 7 showed the temperature dependence of magnetoresistance (MR) ratio for LBMO thin films with thickness of 50 nm. The MR ratio is defined here as $(\rho_0-\rho_H)/\rho_0$ ($\mathrm{H}=0.8\,\mathrm{T}$). With x increasing, the MR peak temperature increases, but the MR peak value $\mathrm{MR}_{\max}$ decreases. As $x=0.05$, large MR effect persists down to low temperature, which may be related to the reemergence of insulating behavior at low temperature in this thickness. As $x=0.1$, $\mathrm{MR}_{\max}$ of about 40% occurs around room temperature under a magnetic field of only 0.8 T. With respect to applications, the $x=0.1$ thin film is most interesting, due to the large room-temperature and low field CMR effect in such a low doping level.

D. Phase diagram

Based on the magnetic and transport properties reported above, a phase diagram of LBMO thin films was constructed and shown in Fig. 8. The T_C of bulk LBMO (for $x=0.05$, spin canting transition temperature T_{CA}) is also plotted as a comparison, and the lattice mismatch between bulk LBMO and STO for each doping level is listed in the top axis. The shadowy region is the ferromagnetic and metallic state of LBMO thin films with thickness of 20 nm. It is obviously shown in this phase diagram that, compared with the bulks, ferromagnetism in LBMO thin film is suppressed by compressive strain, but enhanced by tensile strain. It is the strain effect that produces a new phase diagram, not only different from the bulk one, but also exhibiting some exciting novel properties.

With respect to the application in electronic devices, the low doping level is of high interest. Most notably, room-temperature ferromagnetism was obtained in a CMR material with such a low doping level as $x=0.1$, which enables the $x=0.1$ LBMO thin film to be a promising candidate material in electronic applications. In addition, as shown in the phase diagram, in low doping level (x below 0.1), T_C of LBMO thin films changes greatly with doping level x. In other words, the magnetotransport properties are very sensitive to carrier concentration. This feature will give high sensitivity and efficiency to some electronic devices based on the low doped LBMO thin films, in which carrier concentration is modulated to realize novel performance. One can expect large changes of the magnetic and transport properties in the thin films at room temperature by introducing slight fluctuation in the carrier concentration. Therefore, some new strongly correlated electronic devices can be developed, such as photosensitive device (photocarrier injection effect), magnetic oxide p-n junction, and field effect transistor (FET). Photocarrier control of magnetotransport properties has been observed in $(\mathrm{La,Sr})\mathrm{MnO_3}$/STO heterostructure,[16] and may be more prominent even at room temperature for LBMO based device. Mathews *et al.*[17] have fabricated the ferroelectric FET based on epitaxial perovskite heterostructure $\mathrm{La_{0.7}Ca_{0.3}MnO_3}$/PZT, but the channel resistivity change under poling voltage is still small. If replacing $\mathrm{La_{0.7}Ca_{0.3}MnO_3}$ by $\mathrm{La_{0.9}Ba_{0.1}MnO_3}$, much better performance may be achieved in that FET device. Very recently, we have succeeded in switching ferromagnetism in LBMO ($x=0.1$)/Nb-STO p-n junction through modulating the carrier concentration by applying a low electric field at room temperature.[18] The temperature dependence of the junction resistance shows a metal-insulator transition, whose temperature, corresponding to that of ferromagnetic transition, is hugely modulated from 290 to 340 K by a bias voltage increasing from +1.0 to 1.8 V.

E. Discussion

As proposed above, it is strain effect that results in the novel magnetotransport properties in LBMO thin films. Although the close and clear correlation between structure parameter (lattice strain) and magnetic/transport properties reveals the important and concrete role of strain effect and makes this proposal to be reasonable, some puzzles should be clarified.

In LBMO thin films, tensile strain enhances ferromagnetism, which is different from the usual results in other CMR systems, where tensile strain usually reduces T_C,[5,6] and compressive strain enhances T_C.[10] So, new mechanisms should be responsible for the anomalous strain effect in LBMO thin films. According to double-exchange (DE) mechanism, T_C is proportional to the transfer integral, t_0, of e_g electron hopping between $\mathrm{Mn^{3+}}$ and $\mathrm{Mn^{4+}}$ through Mn-O-Mn network. Tensile strain elongates the in-plane Mn-O bond length d, reducing t_0 (due to $t_0 \propto d^{-3.5}$) and thus T_C; in contrast, compressive strain raises T_C. These are the general understandings of the strain effect. But at the same time, a strain-induced modification of e_g electron orbital stability should be considered. Two orbitals are available for e_g electron, the in-plane $d_{x^2-y^2}$ and out-of-plane $d_{3z^2-r^2}$. In LBMO bulk, electron occupancy in out-of-plane $d_{3z^2-r^2}$ orbital is higher than that in in-plane $d_{x^2-y^2}$ orbital, due to a relatively large c/a ratio, which is related to orbital stability and thus magnetotransport properties.[19,20] In LBMO thin films, an elongation of in-plane Mn-O distance (decrease in c/a) due to tensile strain would stabilize $d_{x^2-y^2}$ orbital, which has a larger transfer intensity than $d_{3z^2-r^2}$ orbital, thus result in increasing of the $d_{x^2-y^2}$ character in the occupied e_g state and the effective in-plane carrier density, which would enhance electron hopping and DE interaction in thin films, and lead to an increase in T_C. In contrast, the compressive strain will suppress ferromagnetism and lead to a decrease in T_C.

So, these two effects, strain-induced modification of Mn-O bond length and e_g orbital stability, are competitive. We suppose that in some CMR system,[5,6,10] the former are dominant; but in LBMO, the latter may be dominant and give rise to the novel properties. In fact, this kind of anomalous strain effect is not exclusively observed in LBMO system, but has been observed in other thin films. In $\mathrm{Pr_{0.5}Ca_{0.5}MnO_3}$/STO thin films,[8] charge-order (CO) state becomes less stable due to tensile strain; and in $\mathrm{La_{0.67}Ca_{0.33}MnO_3/LaAlO_3}$ thin films,[21] CO insulating state is favored by compressive strain, both of which are consistent with the result in our LBMO thin films. These results suggest that this ‘‘anomalous’’ strain effect is probably a general behavior. The important role of the strain-induced modification of orbital stability in LBMO thin films is similar to that of orbital state in layered manganites. Recently, both experimental and theoretical studies confirmed that the relative stability of $3d$ orbitals dominates the magnetic structure and transition temperature of layered manganites, and can be mediated by both chemical and hydrostatic pressures.[22–25] The comparable features of layered manganite and thin film are the reduced dimensionality and the resulted strong anisotropy, which probably dignify the role of orbital stability. A theoretical calculation[20] involving both orbital stability and Mn-O bond length also confirmed that strain effect in different CMR systems can be much different; a tensile strain increases T_C in LBMO system, but reduces T_C in $(\mathrm{La,Ca})\mathrm{MnO_3}$ or $(\mathrm{La,Sr})\mathrm{MnO_3}$ system. These results will probably lead us to orbital physics, a phase control via orbital ordering or orbital polarization due to lattice distortion.

In addition to the strain effect discussed above, another factor should be considered, that is stoichiometry. A possible deviation of $\mathrm{Mn^{3+}/Mn^{4+}}$ ratio in LBMO thin films from that in bulk can lead to a variation in T_C correspondingly. So, we measured the cationic concentration by electronic probe microanalysis (EPMA) for the LBMO bulk and thin films with $x=0.1$. As shown in Fig. 9, EPMA results confirmed a good agreement between the compositions of thin films with different thickness and bulk within error limit. By taking oxygen content to be 3, the derived compositions of the bulk and thin film (averaged value for different thickness) are $\mathrm{La_{0.90}Ba_{0.10}Mn_{0.95}O_3}$ and $\mathrm{La_{0.90}Ba_{0.10}Mn_{0.99}O_3}$, respectively, almost same as the nominal one within the EPMA accuracy. The magnetic properties of LBMO bulk agree very well with the literature result,[12] indicating stoichiometry in LBMO bulk. So, the possibility of significant nonstoichiometry in LBMO thin films can be ruled out. Moreover, both enhancement and suppression of ferromagnetism in different doping level ranges can be well explained only by the proposed strain effect, but not by nonstoichiometry. Therefore, al-

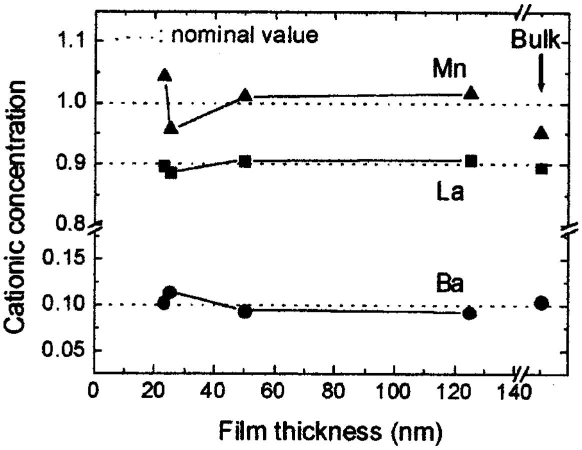

FIG. 9. Cationic concentration of LBMO ($x=0.1$) bulk (target) and thin films with different thickness. Solid line is only a guide for the eyes. Dotted lines indicate the nominal value (Mn: 1.0; La: 0.9; Ba:0.1).

though it is possible that the Mn^{3+}/Mn^{4+} ratio in the thin films is slightly different from that in the bulk, compared with nonstoichiometry, strain effect is the much more reliable origin of the novel properties in LBMO thin films. At least, we cannot attribute the FM enhancement only to the probable slight nonstoichiometry.

One more evidence of strain effect is from the LBMO thin film deposited with a $Sr_{0.8}Ba_{0.2}TiO_3$ ($a=3.933$ Å) buffer layer,[20] which has larger lattice mismatch, i.e., larger tensile strain, and correspondingly shows higher T_C, compared with the film deposited directly on STO. LBMO ($x=0.2$) thin films deposited on STO and SBTO have lattice mismatch of 0.29 and 1.0 %, respectively. At the same thickness, 650 Å, T_C reaches up to 320 K in the latter, while only about 305 K in the former. This result confirmed again the important role of strain effect in LBMO thin films. Based on the above discussion, we argue that it is reasonable to attribute novel magnetic and transport properties in LBMO thin films to strain effect.

IV. SUMMARY

We reported an anomalous strain effect in LBMO/STO thin films, in which tensile strain enhances ferromagnetism and conductivity significantly, and have obtained a phase diagram of the thin films. Room-temperature ferromagnetism was achieved in a very low doping level as $x=0.1$, which is very appealing to the practical applications of CMR thin films. A strain-induced modification of e_g orbital stability was proposed to be responsible for this anomalous strain effect. Our results suggest that external strain can be applied to CMR thin films to produce novel properties absent in the bulk materials, which will illuminate a new way to explore CMR materials with desirable properties for electronic applications.

ACKNOWLEDGMENTS

This work has been performed under the Center of Excellence (COE) program, a Grant-in-Aid for Scientific Research on Priority Area (A), "Novel Quantum Phenomena in Transition Metal Oxides" supported by the Ministry of Education, Culture, Sports, Science and Technology, Japan, and Corning Research Grant. J. Zhang acknowledges the financial support from Japan Society for the Promotion of Science (JSPS).

---

*Author to whom correspondence should be addressed. Electronic address: kawai@sanken.osaka-u.ac.jp

[1] S. Jin, T. H. Tiefel, M. McCormack, H. M. O'Bryan, L. H. Chen, R. Ramesh, and D. Schurig, Appl. Phys. Lett. **67**, 557 (1995).

[2] H. S. Wang, Q. Li, K. Liu, and C. L. Chien, Appl. Phys. Lett. **74**, 2212 (1999).

[3] A. Biswas, M. Rajeswari, R. C. Srivastava, Y. H. Li, T. Venkatesan, R. L. Greene, and A. J. Millis, Phys. Rev. B **61**, 9665 (2000).

[4] F. Tsui, M. C. Smoak, T. K. Nath, and C. B. Eom, Appl. Phys. Lett. **76**, 2421 (2000).

[5] A. J. Millis, T. Darling, and A. Migliori, J. Appl. Phys. **83**, 1588 (1998).

[6] R. A. Rao, D. Lavric, T. K. Nath, C. B. Eom, L. Wu, and F. Tsui, Appl. Phys. Lett. **73**, 3294 (1998).

[7] G. Q. Gong, A. Gupta, G. Xiao, P. Lecoeur, and T. R. McGuire, Phys. Rev. B **54**, R3742 (1996).

[8] W. Prellier, A. M. Haghiri-Gosnet, B. Mercey, Ph. Lecoeur, M. Hervieu, Ch. Simon, and B. Raveau, Appl. Phys. Lett. **77**, 1023 (2000).

[9] R. Shreekala, M. Rajeswari, R. C. Srivastava, K. Ghosh, A. Goyal, V. V. Srinivasu, S. E. Lofland, S. M. Bhagat, M. Downes, R. P. Sharma, S. B. Ogale, R. L. Greene, R. Ramesh, T. Venkatesan, R. A. Rao, and C. B. Eom, Appl. Phys. Lett. **74**, 1886 (1999).

[10] F. S. Razavi, G. Gross, H.-U. Habermeier, O. Lebedev, S. Amelinckx, G. Van Tendeloo, and A. Vigliante, Appl. Phys. Lett. **76**, 155 (2000).

[11] R. von Helmolt, J. Wecker, B. Holzapfel, L. Schultz, and K. Samwer, Phys. Rev. Lett. **71**, 2331 (1993).

[12] H. L. Ju, Y. S. Nam, J. E. Lee, and H. S. Shin, J. Magn. Magn. Mater. **219**, 1 (2000).

[13] Y. Lu, J. Klein, C. Höfener, B. Wiedenhorst, J. B. Philipp, F. Herbstritt, A. Marx, L. Alff, and R. Gross, Phys. Rev. B **62**, 15806 (2000).

[14] T. Kanki, H. Tanaka, and T. Kawai, Solid State Commun. **114**, 267 (2000).

[15] J. Zhang, H. Tanaka, T. Kanki, and T. Kawai, Surf. Interface Anal. **32**, 62 (2001).

[16] H. Katsu, H. Tanaka, and T. Kawai, Appl. Phys. Lett. **76**, 3245 (2000).

[17] S. Mathews, R. Ramesh, T. Venkatesan, and J. Benedetto, Science **276**, 238 (1997).

[18] H. Tanaka, J. Zhang, and T. Kawai (unpublished).

[19] Y. Konishi, Z. Fang, M. Izumi, T. Manako, M. Kasai, H. Kuwahara, M. Kawasaki, K. Terakura, and Y. Tokura, J. Phys. Soc. Jpn. **68**, 3790 (1999).

[20] T. Kanki, H. Tanaka, and T. Kawai, Phys. Rev. B (to be published).

[21] A. Biswas, M. Rajeswari, R. C. Srivastava, T. Venkatesan, R. L.

Green, Q. Lu, A. L. de Lozanne, and A. J. Millis, Phys. Rev. B **63**, 184424 (2001).

[22] T. Akimoto, Y. Moritomo, K. Ohoyama, S. Okamoto, S. Ishihara, S. Maekawa, and A. Nakamura, Phys. Rev. B **59**, R14 153 (1999).

[23] M. Takata, E. Nishibori, K. Kato, M. Sakata, and Y. Moritomo, J. Phys. Soc. Jpn. **68**, 2190 (1999).

[24] Y. Moritomo, K. Hirota, H. Nakao, T. Kiyama, Y. Murakami, S. Okamoto, S. Ishihara, S. Maekawa, M. Kubota, and H. Yoshizawa, Phys. Rev. B **62**, 17 (2000).

[25] S. Okamoto, S. Ishihara, and S. Maekawa, Phys. Rev. B **63**, 104401 (2001).